

2008

Tunable Photonic RF Signal Processor Using Opto-VLSI

Budi Juswardy
Edith Cowan University

Feng Xiao
Edith Cowan University

Kamal Alameh
Edith Cowan University

10.1109/IPGC.2008.4781458

This article was originally published as: Juswardy, B. , Xiao, F. , & Alameh, K. (2008). Tunable Photonic RF Signal Processor Using Opto-VLSI.

PhotonicsGlobal@Singapore, 2008. IPGC 2008. IEEE (pp. 1-4). Singapore. IEEE. Original article available [here](#)

© 2008 IEEE. Personal use of this material is permitted. Permission from IEEE must be obtained for all other uses, in any current or future media, including reprinting/republishing this material for advertising or promotional purposes, creating new collective works, for resale or redistribution to servers or lists, or reuse of any copyrighted component of this work in other works.

This Conference Proceeding is posted at Research Online.

<http://ro.ecu.edu.au/ecuworks/1009>

Tunable Photonic RF Signal Processor Using Opto-VLSI

Budi Juswardy, Feng Xiao, and Kamal Alameh

WA Centre of Excellence for MicroPhotonic Systems, Electron Science Research Institute,
Edith Cowan University, Joondalup, WA, 6027, Australia

Email: f.xiao@ecu.edu.au

Abstract: A tunable photonic RF signal processor is proposed and demonstrated. The filter structure comprises a reconfigurable Opto-VLSI processor for tunability, arrayed waveguide gratings for wavelength slicing and multiplexing, a custom-made fiber array for wavelength routing and dropping, and high-dispersion fibres for true-time delay generation. The processor structure enables positive and negative weights to be synthesised thus realising arbitrary responses. The proof-of-concept of the tunable photonic RF signal processor is experimentally demonstrated.

Index Terms: Photonic RF signal processing, Opto-VLSI, reconfigurable RF systems.

1. Introduction

Photonic-based RF signal processors have the advantages of ultra-wide bandwidth, immunity to electromagnetic interference, flexibility, and light weight in comparison to their all-electronic counterparts. These advantages open new opportunities in a wide range of potential applications if high selectivity or resolution, wide tunability, and fast reconfigurability characteristics are also available [1].

Several reconfigurable photonic RF transversal filter structures have recently been proposed and demonstrated [1-3], where the reconfiguration of the filter transfer function is achieved by adjusting the tap weights through optical attenuation via MEMS switches [2], using variable optical attenuators (VOAs) [4], or employing Fibre Bragg Gratings (FBG) [5] that can be tuned either thermally or mechanically. MEMS switches suffer mechanical reliability issues such as stability and fatigue. The use of VOAs for each spectral taps increases the overall cost, and FBGs are limited in terms of flexibility and tunability. On the other hand, negative coefficients are also necessary to generate a wide range of filter transfer functions. The differential detection technique, which is based on balanced photodetection, allows the synthesis of positive and negative transversal filter weights simultaneously. However, in order to achieve high-resolution reconfigurable photonic RF signal processors that are able to synthesise arbitrary transfer characteristics, extensive research and development is still required [6].

In this paper we propose and demonstrate the principle of a novel reconfigurable photonic RF signal processing structure that employs a broadband optical source, a pair of Arrayed Waveguide Gratings (AWG), an Opto-VLSI

processor, a pair of high-dispersion fibres, and a balanced photodetector to synthesise arbitrarily frequency responses through optical beam steering and multicasting as well as true-time delay generation.

2. Opto-VLSI processor

An Opto-VLSI processor is an array of liquid crystal (LC) cells driven by a Very-Large-Scale-Integrated (VLSI) circuit that generates digital holographic diffraction gratings to steer and/or shape optical beams [7]. Each pixel is assigned a few memory elements that store a digital value, and a multiplexer that selects one of the input voltages and applies it, through the aluminium mirror electrode, across the LC cells. Transparent Indium-Tin Oxide (ITO) is used as the second electrode. The quarter-wave-plate (QWP) layer between the LC and the aluminium mirror is used to accomplish polarization-insensitive operation [8].

The Opto-VLSI processor is electronically controlled, software configurable, polarization independent, and very reliable since beam steering/multicasting is achieved with no mechanically moving part. The deflection angle for the Opto-VLSI processor, α_m , is given by:

$$\alpha_m = \arcsin\left(\frac{m\lambda}{d}\right) \quad (1)$$

where m is the diffracted order (here only first order is considered), λ is the vacuum wavelength, and d is the grating period.

Adaptive optical multicasting can also be achieved for each wavelength channel by uploading an optimised multicasting hologram on the pixel block of the Opto-VLSI processor corresponding to that wavelength channel so that two beams of arbitrary intensities can be diffracted along the axes of the upper and lower fibres [7]. This way, the total number of taps can be doubled, in comparison to the beam steering-only case, leading to improved transfer characteristics. There are several algorithms for the optimization of Opto-VLSI phase holograms to achieve two-way beam splitting, including simulated annealing and projection methods.

3. Photonic RF Processor Structure

The structure of the photonic RF signal processor is shown in Fig. 1. A broadband light source of amplified spontaneous emission (ASE) is externally modulated by the RF signal through an electro-optic modulator (EOM). The

modulated light is routed via a circulator into an N-channel arrayed waveguide grating (AWG 1) that slices the ASE into different RF-modulated wavebands, which are routed to a custom-made fiber array of N fibre pairs. Each fiber pair consists of an upper fiber (connected to an output port of AWG 1) and a lower fiber (connected to a corresponding port of AWG 2). The lower fiber is tilted an angle θ with respect to the upper fiber.

A lens array is used to convert the divergent beams from the upper optical fibers into collimated beams, which illuminate different pixel blocks on the Opto-VLSI active window that is tilted an angle φ with respect to the lens array. When a blank phase hologram is used, the collimated optical beam from an upper optical fiber is reflected off the Opto-VLSI processor and focused through the collimating microlens onto an area between the ends of the upper and lower optical fiber pairs.

By employing an appropriate hologram into the Opto-VLSI processor, the collimated beam is appropriately steered and coupled with arbitrary attenuation (or weight) to either the upper fiber (for positive weights) or to the lower port (for negative weights). Note that the angle θ , between an upper and lower fiber pair, is optimised to minimise the insertion loss and crosstalk that result from switching a collimated beams between the fiber pairs. The wavelengths from the lower ports are multiplexed via AWG 2 and delayed by a high dispersion fiber, while the remaining wavelengths, which are steered and coupled back into the upper fibers, are multiplexed by AWG 1 and reach another similar high dispersion fiber via the circulator. The two multiplexed WDM signals are detected by a pair of balanced photodiodes which generate delayed versions of the input RF signal with positive and negative weights that are controlled by the phase holograms uploaded onto the Opto-VLSI processor, thus realising an arbitrary transfer function.

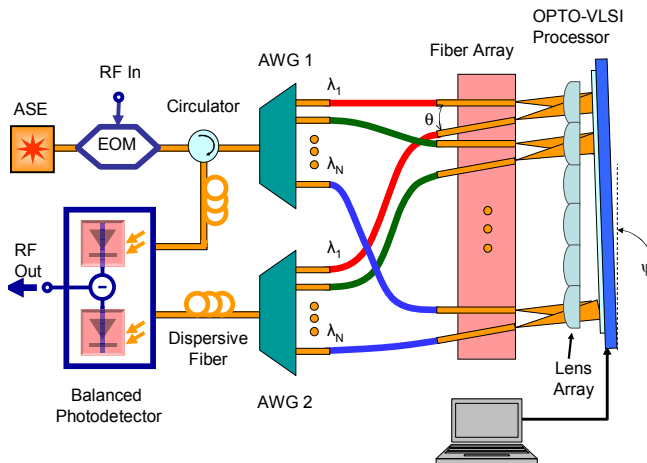


Fig. 1. Novel reconfigurable photonic RF signal processor employing arrayed waveguide gratings, custom-made fiber array, high-dispersion fibers, and an Opto-VLSI processor for synthesising variable filter weights through optical beam steering and multicasting.

4. Simulated Results

The response of the Photonic RF signal processor shown in Fig. 1 can be expressed as

$$H(\omega) = \sum_{k=0}^{N-1} a_k e^{-j\omega k T} - \sum_{k=0}^{N-1} b_k e^{-j\omega k T} \quad (2)$$

where N is the number of the taps, a_k is the weight associated with the optical intensity of the k^{th} waveband, λ_k , coupled into the k^{th} upper optical fibre and detected by the upper photodetector. b_k is the weight associated with the optical intensity of the k^{th} waveband, λ_k , coupled into the k^{th} lower optical fibre and detected by the lower photodetector.

A computer algorithm has been developed to optimise the tap weights, a_k , and b_k that synthesise a specific frequency response and generate the appropriate phase holograms to be uploaded into the Opto-VLSI processor. Fig 2(a) shows simulated 32-waveband dual passband filter response, where only steering holograms are used to generate the filter's 32 weights. Fig 2(b) shows simulated 32-waveband dual passband filter response, where multicasting holograms are used to generate the filter's 64 weights (each waveband is multicast to both of the corresponding fiber pair). It is obvious that weight levels in both Fig. 2(a) and Fig. 2(b) are close in magnitude. However, a much improved filter shape factor is seen when multicasting is employed.

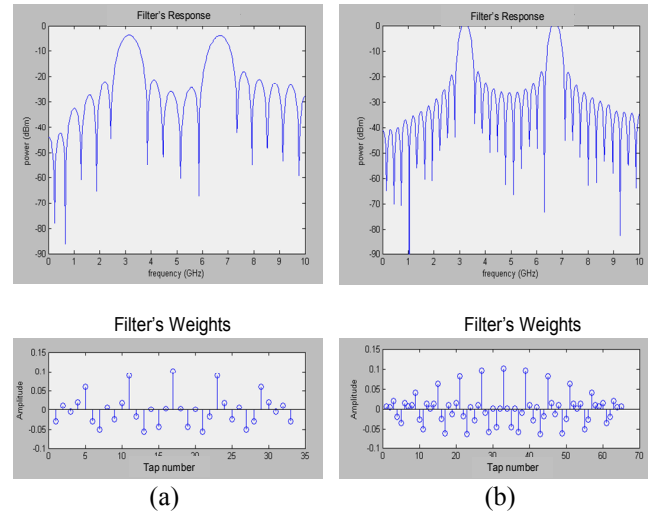


Fig. 2. Examples of filter responses and weights synthesising passbands at 3.1 GHz and 6.7 GHz. (a) 32-waveband (steering only) filter structure, and (b) 32-waveband filter with multicasting.

Fig. 3(a) and Fig. 3(b) show examples of notch filter responses and their corresponding weights where the notch frequency is tuned from 3.1 GHz to 6.7 GHz. Low passband ripples and very high rejection are seen, making the filter structure attractive for many microwave applications, such as the Square Kilometre Array radio telescope and microwave radar.

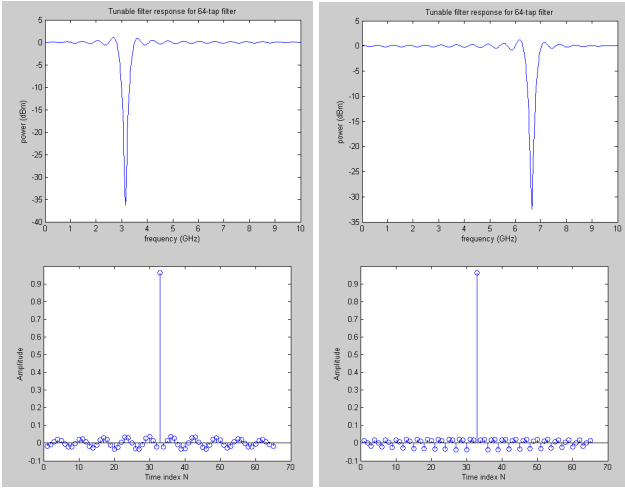


Fig. 3. Notch-filter response and weights of a 64-tap filter structure where the notch frequency is tuned from (a) 3 GHz, to (b) 6.7 GHz.

5. Experiments and results

To demonstrate the principle of the reconfigurable photonic RF signal processor structure, a custom-made fiber array was fabricated with the angle between the upper and lower fiber pairs, θ , being 1.5° . This angle was the optimum that maintains low coupling low and crosstalk between the ports of a fibre pair.

Fig. 4 show the experimental setup used, where a tunable laser source of a tuning range from 1524 nm to 1576 nm was employed in conjunction with two optical spectral analyzers that monitored the positive-coefficient (upper) fiber port and the negative-coefficient (lower) port. A 2mm diameter lens with a focal length of 5 mm was used to collimate the light from the upper fiber at 1mm diameter, and the collimated beam was launched onto the active window of a 256-phase-level one-dimensional Opto-VLSI processor having 1×4096 pixels with $1 \mu\text{m}$ pixel size and $0.8 \mu\text{m}$ dead spacing between adjacent pixels. Labview software was developed to generate the optimized digital holograms that steer or multicast the incident beam along desirable directions.

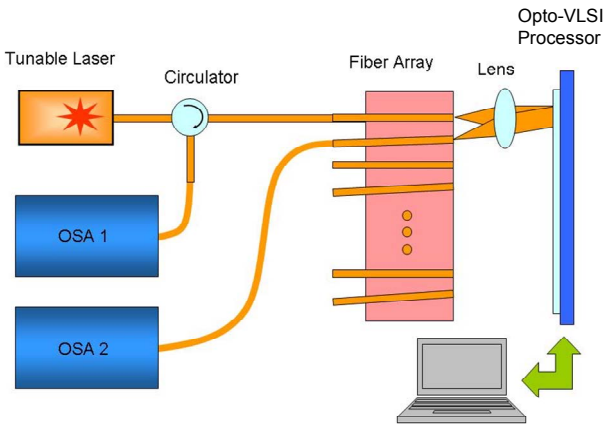


Fig. 4. Experimental setup demonstrating weight synthesis through beam steering and coupling into the upper and lower fiber ports using an Opto-VLSI processor. The fiber array is custom-made and the angle between the upper and lower fiber pair is 1.5° .

When no phase hologram was applied, the Opto-VLSI processor acted like a mirror. Before an appropriate phase hologram was uploaded, the Opto-VLSI processor was slightly tilted so that the reflected collimated beam is focused onto an area between the upper and lower fibers (called zeroth order spot). In the experiment, the zeroth order direction has an angle of 0.61° with respect to the upper fiber, and 0.89° with respect to the lower fiber. Two phase holograms were generated and optimized to steer and couple the incident collimated beam to either the upper fiber (for positive weights) or the lower fiber (for negative weights). The laser power launched into the fiber array was +2 dBm. The maximum intensity coupled to the upper/lower fiber for the positive/negative tap (i.e., the full weight) was -2.9 dBm.

Figs. 5(a) and (b) shows the spectra of the optical signals coupled into the lower and upper fiber ports, using steering holograms intended to couple the wavelengths 1532.9nm and 1530.1nm into the upper port, respectively. The crosstalk (defined as the optical power coupled into the lower fiber port when the optical beam is steered into the upper fiber port) in both steering scenarios is below -40 dB. Fig. 5(c) shows the measured signal and crosstalk levels versus wavelength, demonstrating a maximum crosstalk level below -40 dBm, and hence negligible unwanted fluctuations in the filter's transfer function.

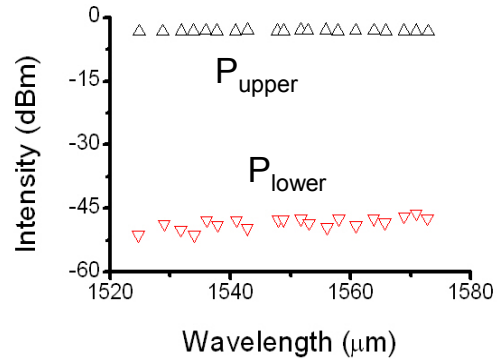
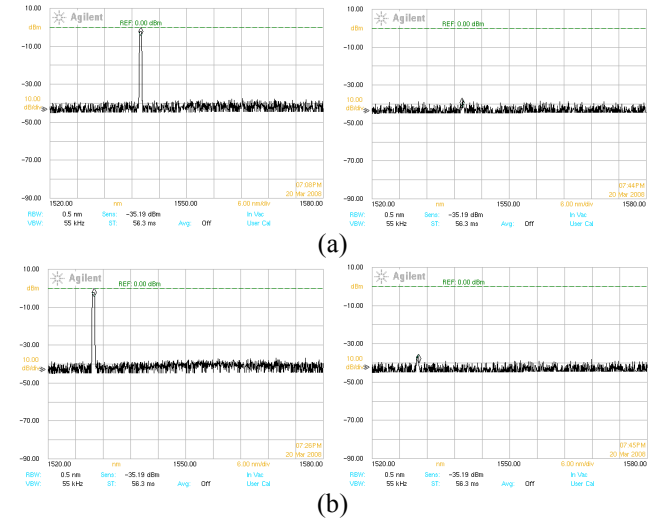


Fig. 5. Maximum optical power coupled into (a) lower port and (b) upper port, versus wavelength. Also shown in Fig. 5(b) is the crosstalk, i.e. the power coupled into the lower port when the optical beam is steered into the upper port.

Note that the Opto-VLSI based reconfigurable photonic RF signal processor has high flexibility in synthesising arbitrary positive and negative weights. This can be achieved by simply reconfiguring the individual steering and multicasting phase holograms uploaded onto the Opto-VLSI processor, thus steering the wavebands and couple them into the appropriate fiber ports. Fig. 6 shows the optical power coupled into the lower fiber port (negative tap) versus the maximum voltage level (which corresponds to a maximum phase level of ψ_{\max}) applied to generate a steering phase hologram. The latter is generally a blazed grating of pitch q pixels and a maximum phase level ψ_{\max} as shown in the inset of Fig. 5, and its diffraction efficiency decreases as ψ_{\max} reduces. It is obvious from Fig. 5 that arbitrary tap weights can be generated by simply adjusting the maximum voltage level applied to the Opto-VLSI processor.

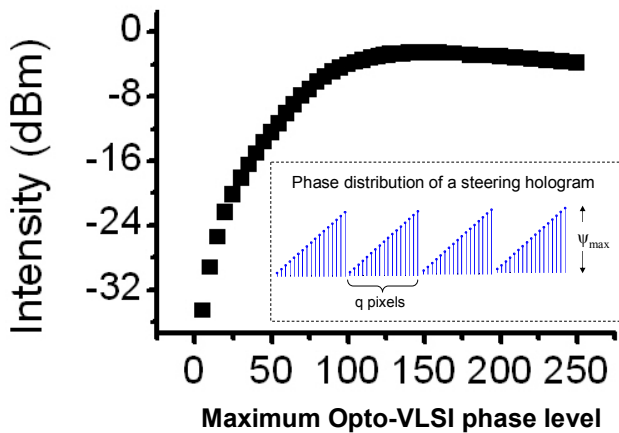


Fig. 6. Coupled optical intensity versus maximum phase level of the Opto-VLSI processor. Inset: An example of a steering blazed grating of period q pixels and maximum optical phase shift ψ_{\max} . A phase level of 256 corresponds to 360° optical phase shift.

The optical coherence that results from the spectral overlapping of adjacent AWG channels was experimentally investigated. Two adjacent wavebands were modulated by the RF signal with one of the bands being delayed with respect to the other band by around 10 ns using a two-meter long optical fiber. The combined RF-modulated bands were detected by a broadband photodetector to realise a two-tap notch filter. The frequency response of the two-tap notch filter was measured by a network analyser at different times, and a stable (fluctuations-free) and repeatable frequency response was observed at the different monitoring times demonstrating negligible optical coherence and insignificant spectral overlapping between adjacent AWG channels.

The experiments described in this paper demonstrate the principle of the reconfigurable photonic RF signal processor. Finally, it is important to note that by employing a two-dimensional $20\text{mm} \times 20\text{mm}$ Opto-VLSI processor, a 512-tap can practically be realised using 128-channel AWGs.

6. Conclusion

We have proposed and demonstrated the principle of a reconfigurable photonic RF signal processor employing arrayed waveguide gratings, a custom-made fiber array, an Opto-VLSI processor, high-dispersion fibers and a balanced photodetector to synthesise arbitrary transfer functions. Simulation and experimental results have demonstrated that arbitrary tap weights can be generated using optimised steering and multicasting phase holograms uploaded onto the Opto-VLSI processor. We have shown that by employing the multicasting capability of the Opto-VLSI processor, the number of filter's taps can be doubled, leading to a much improved filter shape factors in comparison with using a steering-only Opto-VLSI processor. The processor structure has applications in broadband RF signal processing, and potentially in the Square Kilometer Array (SKA) radio telescope [9].

References

- [1] J. Capmany, B. Ortega, and D. Pastor, "A tutorial on microwave photonic filters," *J. Lightw. Technol.*, vol. 24, no. 1, pp. 201–229, Jan. 2006.
- [2] J. Capmany, J. Mora, B. Ortega, and D. Pastor, "Microwave photonic filters using low-cost sources featuring tunability, reconfigurability and negative coefficients," *Opt. Express*, vol. 13, pp. 1412–1417, 2005.
- [3] V. Polo, B. Vidal, J. L. Corral, and J. Marti, "Novel tunable photonic microwave filter based on laser arrays and $N \times N$ AWG-based delay lines," *IEEE Photon. Technol. Lett.*, vol. 15, No. 4, pp. 584–586, 2003.
- [4] D. Pastor, B. Ortega, J. Capmany, S. Sales, A. Martinez, and P. Muñoz, "Optical microwave filter based on spectral slicing by use of arrayed waveguide gratings," *Opt. Lett.*, Vol. 28, pp. 1802–1804, 2003.
- [5] J. D. Taylor, L. R. Chen, and X. Gu, "Simple reconfigurable photonic microwave filter using an array waveguide grating and fiber Bragg gratings," *IEEE Photonics Technology Letters*, vol. 19, pp. 510–512, 2007.
- [6] J. Capmany, B. Ortega, D. Pastor, and S. Sales, "Discrete-time optical processing of microwave signals," *Journal of Light Technology*, Vol. 23, pp. 702–722, 2005.
- [7] Z. Wang, R. Zheng, K. Alameh, R. Robertson, U. Muller, and L. Bloom. "Dynamic optical power splitter using Opto-VLSI processor", *IEE Electronics Letters*, vol. 40, No. 22, pp. 1445–1446, 2004.
- [8] I. G. Manolis, T. D. Wilkinson, M. M. Redmond, and W. A. Crossland, "Reconfigurable multilevel phase holograms for optical switches," *IEEE Photon. Technol. Lett.* 14, 801–803 (2002).
- [9] Steven W. Ellingson, "RFI mitigation and the SKA", *Journal of Experimental Astronomy*, Volume 17, Numbers 1-3 / June, 2004, pp. 261–267.